



## A comparative study of experimental optimization and response surface optimization of Cr removal by emulsion ionic liquid membrane

Rahul Kumar Goyal, N.S. Jayakumar, M.A. Hashim\*

Department of Chemical Engineering, University of Malaya, Malaysia

### ARTICLE INFO

#### Article history:

Received 24 March 2011  
Received in revised form 21 July 2011  
Accepted 19 August 2011  
Available online 26 August 2011

#### Keywords:

Emulsion ionic liquid membrane  
Chromium  
Response surface methodology  
[BMIM]<sup>+</sup>[NTf<sub>2</sub>]<sup>-</sup>  
Optimization

### ABSTRACT

A comparative study on the optimization of process parameters of an emulsion ionic liquid membrane (EILM) by experimental work and response surface methodology (RSM) has been carried out. EILM was prepared by using kerosene as solvent, Span 80 as surfactant, NaOH as internal reagent, a hydrophobic ionic liquid 1-butyl-3-methylimidazolium bis(trifluoromethylsulfonyl)imide ([BMIM]<sup>+</sup>[NTf<sub>2</sub>]<sup>-</sup>) as a stabilizer and a second ionic liquid tri-n-octylmethylammonium chloride (TOMAC) as a carrier. The prepared EILM was used to separate and concentrate Cr from wastewaters. The comparison between the experimentally optimized and the RSM optimized values was accomplished by optimizing the following parameters: homogenization speed, carrier concentration, internal phase concentration, agitation speed, treat ratio, internal to membrane phase ratio, surfactant concentration and pH of the feed phase. The comparison showed that all the values were in good agreement except for the internal phase concentration and the treat ratio. It was observed that the stability provided by [BMIM]<sup>+</sup>[NTf<sub>2</sub>]<sup>-</sup> decreased as the extraction progressed due to its high density. Nevertheless, a good stability could be obtained by the combination of [BMIM]<sup>+</sup>[NTf<sub>2</sub>]<sup>-</sup> and Span 80 during extraction process.

© 2011 Published by Elsevier B.V.

### 1. Introduction

Hexavalent Cr is a very toxic form of the Cr metal compared to trivalent Cr (III) due to its oxidizing nature. Cr (VI) is not only carcinogenic but causes many serious health problems to the biological system such as nose bleeding, respiratory problems, skin rashes, etc. Cr (VI) also affects wild life in a significant amount that has raised serious concerns in our eco-system. World Health Organization has declared Cr (VI) removal from wastewater as a serious and prime research topic in 1998 meeting held in Geneva. The development of new technologies for the removal of Cr is still progressing day by day [1–4].

Emulsion liquid membrane (ELM) has been proven to be a competent extraction technology for the removal of Cr from industrial wastewaters. In this process, a prepared emulsion is dispersed into a feed phase which contains the solute to be removed. Single stage operation and less power consumption make this technology more favorable over pressure-driven membrane process and solvent extraction [5–8]. There are various parameters which affect the efficiency of ELM such as homogenization speed, carrier concentration, internal phase concentration, agitation speed, treat ratio, internal to membrane phase ratio, surfactant concentration, pH of

the feed phase and the concentration of stabilizer. The maximum percentage removal of Cr is obtained when all these parameters have optimized values. These values can be estimated either by experiments involving the variation in the value of one parameter at a time while keeping other parameters at constant values or by using response surface methodology [9–11].

Recent advances in the applications of ionic liquids have drawn a significant attention of researchers all over the world. Room temperature ionic liquids are composed of organic cations and organic or inorganic anions. The physical and chemical properties of RTILs can be modified by changing the cation or anion or both to facilitate a particular task. These properties include negligible vapour pressure, inflammability, thermal stability even at high temperatures and application based adjustable miscibility/immiscibility in chemical processes [12–17]. Ionic liquids possess a very negligible vapour pressure that has enabled them to be used as a “green solvent” in synthesis [15,16,18–20], separation and purification [21–27] and electrochemical application [27].

In our recent work, we have shown that ionic liquid [BMIM]<sup>+</sup>[NTf<sub>2</sub>]<sup>-</sup> acted as a stabilizer in ELM system when kerosene as solvent, Span 80 as surfactant, NaOH (0.1N) as internal phase and TOMAC as carrier was used (article in press, Journal of Hazardous Material). It was found out that 3% (w/w) of [BMIM]<sup>+</sup>[NTf<sub>2</sub>]<sup>-</sup> provided substantial amount of stability during the extraction process with the least possible resistance to the mass transfer of Cr. In this study, EILM (emulsion ionic liquid membrane) has been used to extract Cr from wastewaters.

\* Corresponding author. Fax: +60 3 79675319.  
E-mail address: [alishashim@um.edu.my](mailto:alishashim@um.edu.my) (M.A. Hashim).

Response surface methodology (RSM) has attracted a substantial deal of interest in the past 2–3 decades. It is a statistical tool that is used nowadays very commonly to optimize experimental parameters, to model and to analyze a response of interest. RSM not only provides the optimum level for each variable but also estimates interactions among them and their impact on one or more measured responses [28,29]. This methodology cuts down the number of experiments by a substantial amount without affecting the interactions among the parameters. RSM has been utilized to optimize the parameters of several biotechnological processes such as fermentation, biosorption of metals, oxidation and catalyzed reaction conditions [30–32]. It has also been a useful tool to optimize widely employed parameters such as temperature, pH, stirring speed, concentration of various phases, and aeration rate in several processes [33–36].

In literature, there is not much work available on the comparison between the experimental and RSM optimization of Cr removal by EILM. Therefore, a statistical optimization of the parameters such as homogenization speed, carrier concentration, internal phase concentration, agitation speed, treat ratio, internal to membrane phase ratio, surfactant concentration, pH of the feed phase was carried out to study the individual and interactive effects of parameters on the extraction of Cr using ELM, and the optimized values were compared with the values obtained from the individual experimental optimization of the parameters.

## 2. Materials and methods

### 2.1. Chemicals

All the chemicals described here were used without any further purification. Ionic liquids [BMIM]<sup>+</sup>[NTf<sub>2</sub>]<sup>-</sup> and TOMAC were procured from Merck (Germany). Span 80 a non-ionic surfactant was kindly supplied by Merck (Malaysia). ACROS (USA) kindly provided kerosene of boiling point ranged from 180 to 280 °C. Sodium hydroxide pellets, potassium dichromate and hydrochloric acid were obtained from R&M Chemicals (UK). The solution of sodium hydroxide of desired normality was prepared by dissolving appropriate weight of pellets in de-ionized water. Similarly, Cr solution of 100 mg/L was prepared by mixing suitable amount of potassium dichromate in de-ionized water.

### 2.2. Analytical instruments

The preparation of emulsion was carried out using a high speed homogenizer (IKA, model: T25 digital Ultra Turrax) and subsequently it was dispersed in the feed phase by using a stirrer (IKA, model: RW11 Lab Egg). An ICP-spectrophotometer (PerkinElmer, model: Optima 7000 DV) was used for the measurement of the Cr concentration. pH of the feed phase was quantified using a Cyber-Scan 510 pH meter.

### 2.3. Procedure

#### 2.3.1. Preparation of emulsion

The emulsion was prepared in a 100 mL beaker by mixing organic solvent, an appropriate amount of Span 80, TOMAC and [BMIM]<sup>+</sup>[NTf<sub>2</sub>]<sup>-</sup>. The mixture was homogenized for up to 5 min. The drops of NaOH were added into the mixture by using a syringe, keeping the whole mixture homogenized for the next 5 min. Hence, we obtained the emulsion which appears as a milky white homogeneous solution.

#### 2.3.2. Extraction of chromium

The prepared emulsion was poured into another 250 mL beaker containing the feed phase. The mixture was stirred gently by using a

**Table 1**  
Factors and their corresponding values.

Factors	Levels		
	-1	0	1
Homogenization speed (rpm), $X_1$	4000	7000	10,000
Internal phase concentration (% w/w), $X_2$	0.05	0.525	1
Carrier concentration (% w/w), $X_3$	0.1	0.3	0.5
Surfactant concentration (% w/w), $X_4$	1	3	5
pH of the feed phase, $X_5$	0.2	1.1	2
Agitation speed (rpm), $X_6$	100	250	400
Treat ratio, $X_7$	1	2	3
Internal to organic phase ratio, $X_8$	0.25	0.625	1

mechanical stirrer with the speed in the range of 200–400 rpm. The pH of the feed phase was initially taken lower than 2 to establish a pH difference between the stripping and the feed phase. Samples were taken on a regular interval by using syringes and the syringes were kept undisturbed for some time until the emulsion and the feed phase were separated. The feed phase was then taken out, filtered and analyzed using ICP-spectrophotometer.

## 3. Results and discussion

Design-Expert 7.16 software was used to analyze the data and to estimate the coefficients of the regression equation. An orthogonal 2<sup>4</sup> Box–Behnken design (BBD) having five replicates at the centre point was used to estimate the coefficients of the response function which is a second order polynomial as given by Eq. (1). It resulted in 29 experiments for four variables.

$$Y = \beta_0 + \sum_{i=1}^k \beta_i X_i + \sum_{i=1}^k \beta_i X_i^2 + \sum_{i < j}^k \sum_j \beta_{ij} X_i X_j + \dots \quad (1)$$

where  $Y$  is the predicted response,  $\beta_i$ ,  $\beta_j$ , and  $\beta_{ij}$  are the coefficients estimated from regression,  $X_i$  is the uncoded value of the  $i$ th variable,  $i$  is the linear coefficient,  $j$  is the quadratic coefficient, and  $k$  is the number of factors.

Due to the large number of variables, two sets of four variables each were formed, and are described as following:

Set-I	Set-II
Homogenization speed (rpm), $X_1$	pH of the feed phase, $X_5$
Internal phase concentration (% w/w), $X_2$	Agitation speed (rpm), $X_6$
Carrier concentration (% w/w), $X_3$	Treat ratio, $X_7$
Surfactant concentration (% w/w), $X_4$	Internal to organic phase ratio, $X_8$

The effect of ionic liquid [BMIM]<sup>+</sup>[NTf<sub>2</sub>]<sup>-</sup> concentration on the removal of Cr was found to be insignificant experimentally. Therefore, it has been excluded from the parameter list. The coded and uncoded values, different levels and the range of the variables are given in Table 1

### 3.1. Interactions and optimization of the variables of set-I

Box–Behnken design matrix for the set-I is given in Table 2 along with the experimental and the predicted response. The percentage removal efficiency of Cr was considered as the predicted response in DoE. Experiments were conducted in the same sequence as they are provided in the table, keeping all other four variables at constant values. pH of the feed phase was maintained at 0.5 while agitation speed of 300 was fixed to achieve the maximum surface area. Treat ratio ( $F/E$ ) and internal to organic phase ratio ( $I/O$ ) were kept at the value of 2 and 1/3, respectively.

The corresponding coefficients of Eq. (1) for this set were obtained by regression analysis of the experimental data, and the equation in decoded form is shown in Eq. (2). In the equation, only the significant variables are included.

**Table 2**  
Box–Behnken design matrix for set-I.

Run	X <sub>1</sub>	X <sub>2</sub>	X <sub>3</sub>	X <sub>4</sub>	% Removal of Cr	
					Experimental	Predicted
1	0	-1	0	-1	75.56	75.90
2	-1	0	0	-1	74.34	74.33
3	0	0	0	0	93.86	93.59
4	-1	-1	0	0	84.56	83.91
5	0	0	0	0	93.43	93.59
6	0	0	0	0	93.44	93.59
7	0	0	1	1	76.45	75.91
8	1	0	0	-1	83.76	84.00
9	-1	0	1	0	82.45	82.72
10	0	-1	-1	0	80.43	80.02
11	-1	0	0	1	83.54	83.22
12	0	0	0	0	93.3	93.59
13	-1	1	0	0	78.61	78.86
14	1	0	0	1	77.45	77.37
15	1	-1	0	0	81.63	81.11
16	0	-1	1	0	76.32	76.43
17	0	-1	0	1	75.43	76.57
18	0	1	0	-1	75.89	75.11
19	0	0	-1	1	76.34	76.12
20	-1	0	-1	0	78.34	78.81
21	1	0	-1	0	79.01	79.10
22	0	1	-1	0	70.76	70.57
23	1	1	0	0	85.1	85.48
24	0	1	0	1	76.67	76.69
25	0	0	-1	-1	68.98	69.25
26	0	1	1	0	84.89	85.21
27	1	0	1	0	86.35	86.24
28	0	0	1	-1	80.56	80.51
29	0	0	0	0	93.94	93.59

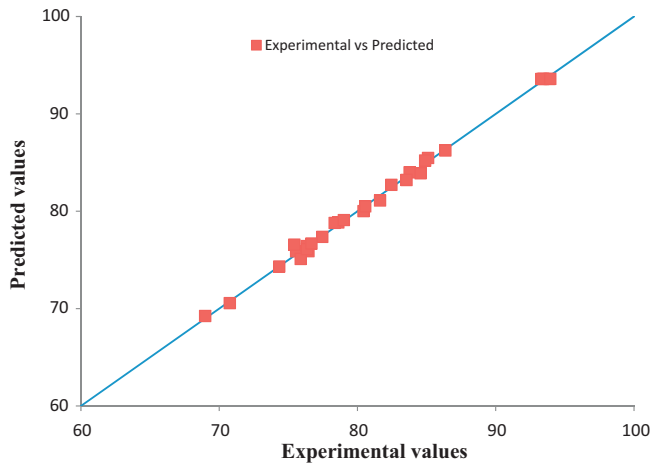


**Fig. 1.** Predicted vs. experimental values for set-I.

$$\begin{aligned}
 Y = & 93.59 + 0.95 * X_1 + 2.76 * X_3 + 0.57 * X_4 - 3.80 * X_1^2 \\
 & - 7.46 * X_2^2 - 8.08 * X_3^2 - 10.07 * X_4^2 + 2.36 * X_1 * X_2 \\
 & + 0.81 * X_1 * X_3 + 3.88 * X_1 * X_4 + 4.56 * X_2 * X_3 \\
 & - 2.87 * X_3 * X_4 \quad (2)
 \end{aligned}$$

where Y is the percentage removal efficiency of Cr by ELM, X<sub>1</sub> is the homogenization speed, X<sub>2</sub> is the internal phase concentration, X<sub>3</sub> is the carrier concentration and X<sub>4</sub> is the surfactant concentration. The predicted values calculated from Eq. (2) were in very good agreement with the experimental values, as shown in Fig. 1. Hence, this quadratic model is well suited for this experimental set up.

However, the significance and the fitness of the model was verified by using statistical test widely known as ANOVA (analysis of variance). ANOVA also helps to check the validity of the equation. ANOVA results are illustrated in Table 3.

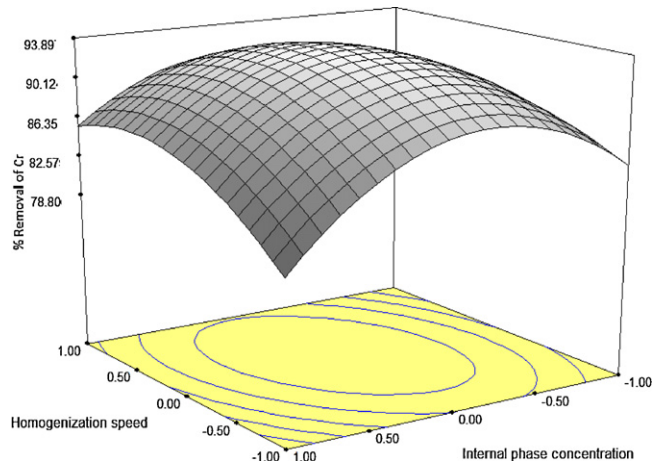


**Fig. 2.** Response surface plot for the interaction between the homogenization speed and the internal phase concentration.

The Model F-value of 304.56 implies that the model is significant. There is only a 0.01% chance that a “Model F-value” this large could occur due to noise. Values of “prob > F” less than 0.0500 indicate model terms are significant and the rest are considered as insignificant. In this case X<sub>1</sub>, X<sub>3</sub>, X<sub>4</sub>, X<sub>1</sub><sup>2</sup>, X<sub>2</sub><sup>2</sup>, X<sub>3</sub><sup>2</sup>, X<sub>4</sub><sup>2</sup>, X<sub>1</sub>X<sub>2</sub>, X<sub>1</sub>X<sub>3</sub>, X<sub>1</sub>X<sub>4</sub>, X<sub>2</sub>X<sub>3</sub>, X<sub>3</sub>X<sub>4</sub> are significant model terms. Values greater than 0.1000 indicate the model terms are not significant. The “Lack of Fit F-value” of 5.08 implies that it is not significant in comparison with the pure error. There is a 6.56% chance that a “Lack of Fit F-value” this large could occur due to noise. It is always necessary to have the value of “Lack of Fit F-value” non significant to make the model best fit.

Predicted R<sup>2</sup> represents the prediction of a response value estimated by the model. The difference between adjusted R<sup>2</sup> and predicted R<sup>2</sup> is always wanted to be in the range of 0–0.200 for the adequacy of the model. In this case, the difference between them is 0.0113 which implies that both the values are in good agreement.

Adequate Precision is an estimation of the signal to noise ratio. A ratio greater than 4 is desirable. The ratio of 59.787 implies an adequate signal. Hence, this model can be used to navigate the design space. Coefficient of variation indicates the error expressed as a percentage of the mean.

The response surface curves indicate the interaction of the variables and also determine the optimum level of variables for maximum response. The response surface plots for significant interaction between two variables against % removal efficiency of Cr by EILM are, as shown in Figs. 2–6.

### 3.2. Significant interactions of the variables of set-I

The contour plot in Fig. 2 illustrates the interaction between the homogenization speed and the internal phase concentration/NaOH concentration. In the figure, the parabolic nature of contours implies that the interaction between both the variables is significant. The homogenization speed and the internal phase concentration, both cause the increase in the % removal efficiency when their values were increased from lower level to up to a certain point. After this point, the % removal efficiency decreases, as illustrated in Fig. 2. The optimized values are provided in Section 3.3. The interaction between the homogenization speed and the internal phase concentration can be explained by the fact that the viscosity is directly proportional to internal phase concentration, and the internal phase droplet size is dependent on the viscosity and the homogenization speed. Thus, they are inter-related.

**Table 3**  
ANOVA for response surface model of set-I.

Source	Sum of squares	DF	Mean square	F-value	P-value, prob > F	
Model	1366.76	14	97.63	304.56	<0.0001	significant
X <sub>1</sub>	10.94	1	10.94	34.14	<0.0001	
X <sub>2</sub>	0.34	1	0.34	1.05	0.3228	
X <sub>3</sub>	91.63	1	91.63	285.86	<0.0001	
X <sub>4</sub>	3.84	1	3.84	11.99	0.0038	
X <sub>1</sub> <sup>2</sup>	93.52	1	93.52	291.74	<0.0001	
X <sub>2</sub> <sup>2</sup>	360.81	1	360.81	1125.63	<0.0001	
X <sub>3</sub> <sup>2</sup>	423.43	1	423.43	1320.96	<0.0001	
X <sub>4</sub> <sup>2</sup>	657.53	1	657.53	2051.30	<0.0001	
X <sub>1</sub> X <sub>2</sub>	22.18	1	22.18	69.21	<0.0001	
X <sub>1</sub> X <sub>3</sub>	2.61	1	2.61	8.14	0.0128	
X <sub>1</sub> X <sub>4</sub>	60.14	1	60.14	187.62	<0.0001	
X <sub>2</sub> X <sub>3</sub>	83.17	1	83.17	259.48	<0.0001	
X <sub>2</sub> X <sub>4</sub>	0.21	1	0.21	0.65	0.4350	
X <sub>3</sub> X <sub>4</sub>	32.89	1	32.89	102.61	<0.0001	
Residual	4.49	14	0.32			
Lack of Fit	4.16	10	0.42	5.08	0.0656	not significant
Pure error	0.33	4	0.082			
Cor Total	1371.25	28				

Std. deviation: 0.57; mean: 81.43; coefficient of variation: 0.70; R-squared: 0.9967; adjusted R-squared: 0.9935; predicted R-squared: 0.9822; adequate precision: 59.787

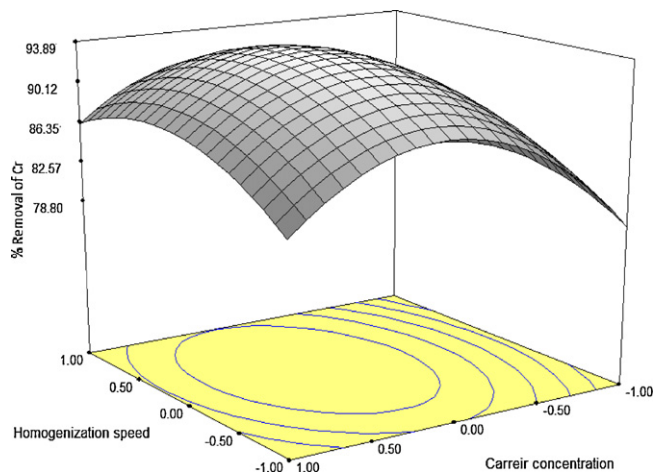


**Fig. 3.** Response surface plot for the interaction between homogenization speed and the carrier concentration.

The interaction between the homogenization speed and the carrier concentration is, as shown in Fig. 3. Parabolic contours signify that the interaction between them is significant. The curve illustrates that both the values increase the % removal efficiency upon

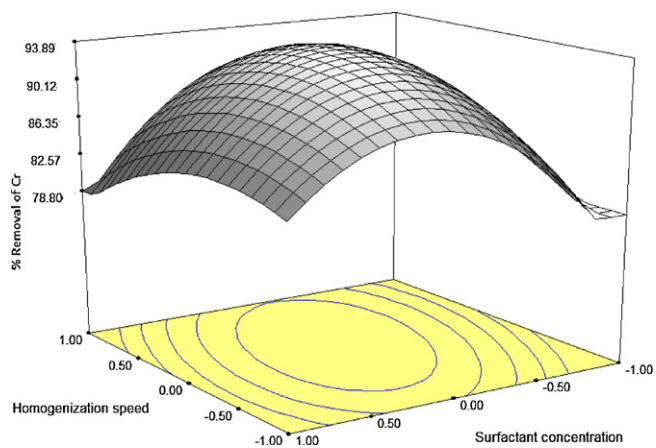


**Fig. 4.** Response surface plot for the interaction between the homogenization speed and the surfactant concentration.

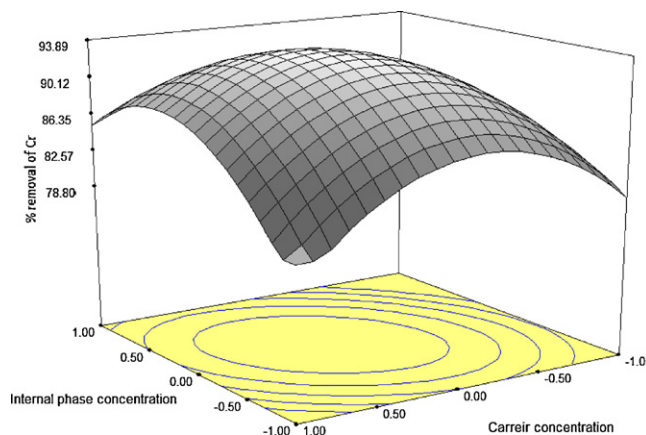


**Fig. 5.** Response surface plot for the interaction between the internal phase concentration and the carrier concentration.

increment from lower level, but after certain values, the % removal efficiency tend to decline until the higher level. The optimum values can be found out easily since the contours are parabolic. The reason for significant interaction can be given as the viscosity of EILM is dependent on the carrier concentration, and the small sized globules formation is dependent on the viscosity and

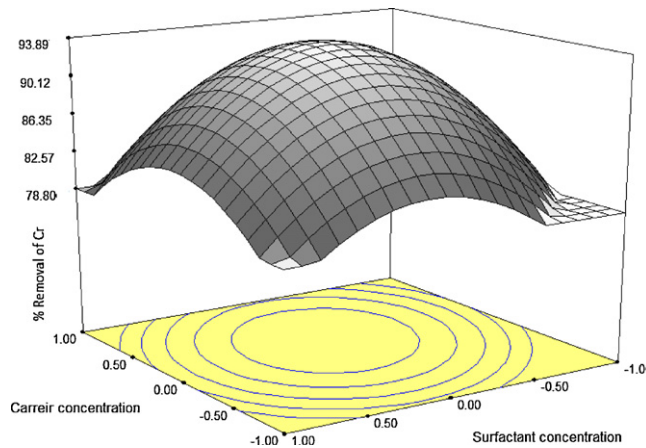


**Fig. 6.** Response surface plot for the interaction between the carrier concentration and the surfactant concentration.

homogenization speed. TOMAC increases the viscosity of EILM that hinders the effect of the homogenization speed in order to form the small size globules.

Fig. 4 demonstrates the interaction between the homogenization speed and the surfactant concentration. % removal of Cr increases upon increasing the concentration of Span 80 up to a certain value. However, it decreases with further increment. Similar kind of results were obtained for the homogenization speed meaning that both are having optimum values at which maximum % removal can be achieved. Since contours are parabolic, the interaction between them is significant. The reason for the significant interaction can be provided by the nature of the surfactant which helps to protect the internal droplets from high shear and stress caused by homogenization speed. Surfactant concentration also contributes in making fine droplets of internal phase under a reasonable homogenization speed.

Interaction between the internal phase concentration and the carrier concentration is illustrated in Fig. 5. It can be observed from the figure that the contours are parabolic, which indicates that the interaction is significant. % removal of Cr increases upon increasing the values of both the parameters from the lower range up to certain values. After these values, the % removal of Cr decreases. The significance of the interaction can be explained by the reaction between TOMAC and NaOH which takes place at the inner interface. The reaction not only affects the stripping reactions but also the overall removal efficiency. Another important interaction between them is the fight for the limiting reagent, since carrier and internal phase are involved in the extraction and stripping reaction, respectively. Hence, they are highly interactive parameters in EILM process.

Fig. 6 shows the interaction between the carrier concentration and the surfactant concentration. Circular contours of the figure imply that the interaction between the parameters is not significant. Hence, the optimum values of the variables are not easy to find. However, increasing the surfactant concentration and carrier concentration increases the % removal efficiency up to certain values. After that, the removal efficiency decreases upon further increment in both the values. The trend of the curve is more or less similar to the ones described earlier for other variables' interactions except the contours.

### 3.3. Optimization of the variables of set-I

The statistical optimization of all four parameters was done by design of experiments (DoE) 7.04. DoE resulted in 10 different solutions with having % removal of Cr almost same in all of them. However, the solution with minimum carrier concentration was selected, since it is the most expensive chemical in comparison with the rest. The coded values of the homogenization speed, the internal phase concentration, the carrier concentration and the surfactant concentration are 0.22, 0.05, 0.18 and  $-0.03$ , respectively. The % removal efficiency was predicted at the value of 93.94% under these optimized values. The uncoded values for the homogenization speed and the internal phase concentration were calculated from coded values are 7660 rpm and 0.548 M, respectively. Similarly, the carrier concentration and the surfactant concentration are 0.336 and 3.06% (w/w), respectively.

All the optimum values are in good agreement with the experimental optimization except for the value of the internal phase concentration. The reason for this discrepancy may be given as the large value range chosen (0.05–1 M) for the internal phase concentration. However, model results are significant and well suited with the experimental results.

**Table 4**  
Box–Behnken design matrix for set-II.

Run	$X_1$	$X_2$	$X_3$	$X_4$	% Removal of Cr	
					Experimental	Predicted
1	-1	0	0	1	85.43	87.20
2	0	0	0	0	94.69	94.49
3	0	-1	-1	0	69.45	68.97
4	1	-1	0	0	50.23	50.36
5	0	-1	0	-1	73.48	75.13
6	0	0	1	1	89.92	89.02
7	1	1	0	0	48.29	50.83
8	0	0	-1	1	70.69	70.95
9	1	0	0	-1	55.45	53.21
10	0	1	-1	0	78.43	77.38
11	0	0	0	0	95.02	94.49
12	0	0	1	-1	78.43	78.35
13	0	0	0	0	93.7	94.49
14	0	0	0	0	95.32	94.49
15	0	-1	1	0	78.64	79.22
16	-1	-1	0	0	79.41	77.05
17	1	0	-1	0	44.98	44.83
18	0	1	1	0	84.12	84.13
19	1	0	1	0	56.32	56.27
20	0	0	0	0	93.72	94.49
21	0	1	0	1	84.26	82.90
22	-1	0	1	0	85.78	86.22
23	0	-1	0	1	76.68	77.15
24	0	0	-1	-1	78.33	79.41
25	0	1	0	-1	82.89	82.71
26	-1	0	0	-1	84.01	83.78
27	-1	1	0	0	89.87	89.91
28	-1	0	-1	0	80.32	80.66
29	1	0	0	1	52.23	51.99

### 3.4. Interactions and optimization of the variables of set-II

Similarly, Box–Behnken design matrix for the set-II was obtained by DoE 7.04 and is given in Table 4. Experiments were conducted in the same sequence as they are provided in the table, keeping all other four variables at constant optimized values as predicted by set-I analysis. The homogenization speed was maintained at 7660 rpm while the internal phase concentration of the value of 0.548 M was fixed to achieve the optimum stripping reagent. The carrier concentration and the surfactant concentration of the values of 0.336 and 3.06% (w/w) were taken respectively, to carry out the experiments.

The corresponding coefficients of Eq. (1) for this set were obtained by regression analysis of the experimental data, and it is shown in Eq. (3) in decoded form. In the equation, insignificant terms are discarded and only significant terms have been included:

$$Y = 94.49 - 16.44 * X_5 + 3.33 * X_6 + 4.25 * X_7 - 18.94 * X_5^2 - 8.51 * X_6^2 - 8.55 * X_7^2 - 6.50 * X_8^2 - 3.10 * X_5 * X_6 + 4.78 * X_7 * X_8 \quad (3)$$

where Y is the percentage removal efficiency of Cr by ELM,  $X_5$  is the pH of the feed phase,  $X_6$  is the agitation speed,  $X_7$  is the treat ratio and  $X_8$  is the internal to membrane phase ratio.

The predicted values calculated from Eq. (2) were in very good agreement with the experimental values, as shown in Fig. 7. Hence, this quadratic model is well suited for this experimental set up.

Furthermore, the validation and the fitness of the model were affirmed by ANOVA (analysis of variance). ANOVA results are shown in Table 5.

The Model F-value of 202.94 implies that the model is significant. There is only a 0.01% chance that a "Model F-value" this large could occur due to noise. Values of "prob > F" less than 0.0500 indicate model terms are significant and the rest are considered as insignificant. In this case  $X_5$ ,  $X_6$ ,  $X_7$ ,  $X_5^2$ ,  $X_6^2$ ,  $X_7^2$ ,  $X_8^2$ ,  $X_5X_6$  and  $X_7X_8$

**Table 5**  
ANOVA for response surface model of set-II.

Source	Sum of squares	DF	Mean square	F-value	P-value, prob > F	
Model	6374.46	14	455.32	202.94	<0.0001	significant
X <sub>5</sub>	3244.60	1	3244.60	1446.14	<0.0001	
X <sub>6</sub>	133.13	1	133.13	59.34	<0.0001	
X <sub>7</sub>	216.84	1	216.84	96.64	<0.0001	
X <sub>8</sub>	3.65	1	3.65	1.63	0.2228	
X <sub>5</sub> <sup>2</sup>	2326.86	1	2326.86	1037.10	<0.0001	
X <sub>6</sub> <sup>2</sup>	469.89	1	469.89	209.43	<0.0001	
X <sub>7</sub> <sup>2</sup>	474.59	1	474.59	211.53	<0.0001	
X <sub>8</sub> <sup>2</sup>	274.48	1	274.48	122.34	<0.0001	
X <sub>5</sub> X <sub>6</sub>	38.44	1	38.44	17.13	0.0010	
X <sub>5</sub> X <sub>7</sub>	8.64	1	8.64	3.85	0.0699	
X <sub>5</sub> X <sub>8</sub>	5.38	1	5.38	2.40	0.1437	
X <sub>6</sub> X <sub>7</sub>	3.06	1	3.06	1.36	0.2622	
X <sub>6</sub> X <sub>8</sub>	0.84	1	0.84	0.37	0.5511	
X <sub>7</sub> X <sub>8</sub>	91.49	1	91.49	40.78	<0.0001	
Residual	31.41	14	2.24			
Lack of Fit	29.18	10	2.92	5.24	0.0622	not significant
Pure error	2.23	4	0.56			
Cor Total	6405.87	28				

Std. deviation: 50; mean: 76.90; coefficient of variation: 1.95; R-squared: 0.9951; adjusted R-squared: 0.9902; predicted R-squared: 0.9732; adequate precision: 46.096.

are significant model terms. Values greater than 0.1000 indicate the model terms are not significant. The “Lack of Fit F-value” of 5.24 implies that it is not significant in comparison with the pure error. There is a 6.22% chance that a “Lack of Fit F-value” this large could occur due to noise. It is always necessary to have the value of “Lack of Fit F-value” non significant to make the model best fit.

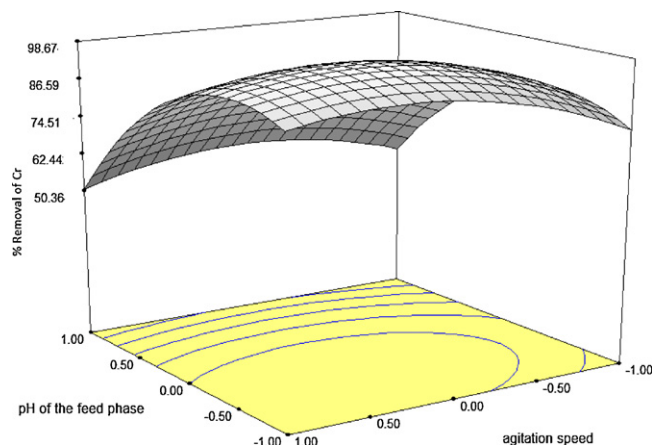
Predicted  $R^2$  represents the prediction of a response value estimated by the model. The difference between adjusted  $R^2$  and predicted  $R^2$  is always wanted to be in the range of 0–0.200 for the adequacy of the model. In this case, the difference between them is 0.0173 which implies that both the values are in good agreement.

Adequate precision is an estimation of the signal to noise ratio. A ratio greater than 4 is desirable. The ratio of 46.096 implies an adequate signal. Hence, this model can be used to navigate the design space. Coefficient of variation indicates the error expressed as a percentage of the mean.

### 3.5. Significant interactions of the variables of set-II

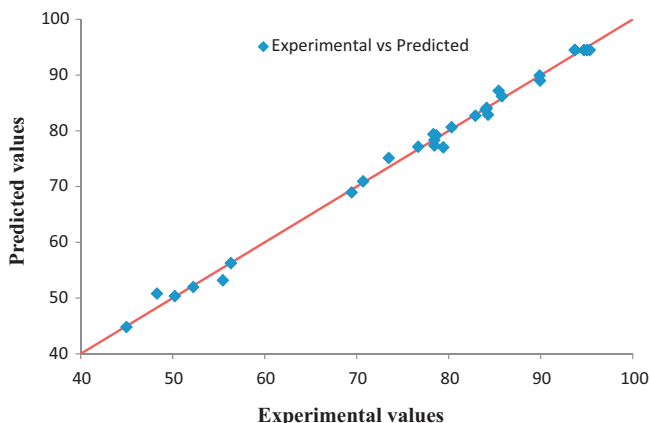
There were only two significant interactions for set-II, as previously shown by ANOVA. One was the interaction between the pH of the feed phase and the agitation speed and the other one was between the treat ratio and the internal to membrane phase ratio. The response curves of both are shown in Figs. 8 and 9.

Fig. 8 describes the interaction of pH of the feed phase and the agitation speed. Since contours of the curve are parabolic, it implies



**Fig. 8.** Response surface plot for the interaction between the pH of the feed phase and the agitation speed.

that the interaction is significant and the optimum values can be calculated easily. % removal of Cr increases upon decreasing the pH of the feed phase but after a certain value, the removal decreases with the further decrease in pH. Similar kind of trend can also be observed for agitation speed. It implicates that both are having



**Fig. 7.** Predicted vs. experimental values for set-II.

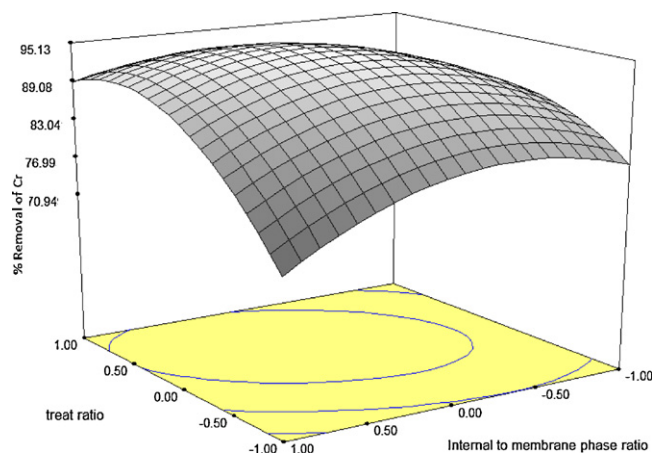


**Fig. 9.** Response surface plot for the interaction between the treat ratio and the internal to membrane phase ratio.

**Table 6**  
Comparison of experimentally optimized values and RSM optimized values.

Parameter	Experimentally optimized	RSM optimized
Homogenization speed (rpm)	8000	7660
Internal phase concentration (M)	0.1	0.548
Carrier concentration (% w/w)	0.3	0.336
Surfactant concentration (% w/w)	3.0	3.06
pH of the feed phase	0.5	0.425
Agitation speed (rpm)	300	296.5
Treat ratio	2	2.60
Internal to membrane phase ratio	0.337	0.715

certain optimum values on which maximum removal of Cr can be achieved.

Physically, the interaction between the pH of the feed phase and the agitation speed can be explained by the fact that the swelling in EILM is caused by the pH of the feed phase and by the agitation speed also. Therefore, swelling acts as a mediator to regulate the interaction between them. The osmotic pressure difference between the internal and the feed phase is also dependent on the pH of the feed phase and the agitation speed. This may also act as a connecting parameter for this interaction.

Fig. 9 shows the interaction between the treat ratio and the internal to membrane phase ratio. Parabolic contours signify that the interaction is quite significant. From the figure it can be predicted that the increment in the treat ratio increases the % removal of Cr up to the upper level while internal to membrane phase ratio achieves maxima in between the lower and the upper level. The possible reason for the interaction can be provided as the direct proportionality of the internal to membrane phase ratio to the treat ratio.

An increment in the internal to membrane phase ratio increases the volume of ELM, and hence decreases the treat ratio. Therefore, they have a good interaction for ELM process.

### 3.6. Optimization of the variables of set-II

The statistical optimization of all four parameters was done by design of experiments (DoE) 7.04. DoE resulted in 10 different solutions with having % removal of Cr up to 97.5. However, the solution with the maximum treat ratio has been selected to economize the ELM process. The coded values of the pH of the feed phase, the agitation speed, the treat ratio and the internal to membrane phase ratio are  $-0.75$ ,  $0.31$ ,  $0.60$  and  $0.24$ , respectively. The % removal efficiency was predicted at the value of 96.38% under these optimized values. The uncoded values for the pH of the feed phase and the agitation speed were calculated from coded values are 0.425 and 296.5 rpm, respectively. Similarly, the treat ratio and the internal to membrane phase ratio of the values of 2.60 and 0.715 respectively were obtained after converting coded values to uncoded values.

All the above optimum values were found to be in good agreement with the experimental optimization, except for the value of the treat ratio. However, model results are significant and well suited with the experimental results.

Table 6 shows that comparison of the optimized values calculated experimentally and by RSM. It shows that the all the values are in good agreement except for the internal phase concentration and the treat ratio. This difference is dependent on the range and levels defined for RSM, swelling of ELM and other experimental errors. However, the model can be used to predict the % removal of Cr by ELM.

## 4. Conclusion

An emulsion ionic liquid membrane (EILM) was prepared using two ionic liquids, i.e. TOMAC as an extractant and  $[BMIM]^+[NTf_2]^-$  as a stabilizer for the separation of Cr. The parameters such as carrier concentration, internal phase concentration, agitation speed, treat ratio, internal to membrane phase ratio, surfactant concentration and pH of the feed phase were optimized separately by individual experimental work and by response surface methodology. The comparison between two optimized values showed that they were in good agreement except for the internal phase concentration and the treat ratio. Interaction between two parameters suggested their inter-dependence on each other and their effect on the final percentage removal of Cr. An effort to lessen the use of organic solvent was made to economize ELM process and to make it more environmentally friendly. Ionic liquid  $[BMIM]^+[NTf_2]^-$  hinders mass transfer of Cr by its polymeric form but the effect was quite insignificant.

### List of symbols

$F/E$	feed to emulsion phase ratio
$I/O$	internal to organic phase ratio
$X_1$	homogenization speed (rpm)
$X_2$	internal phase concentration (% w/w)
$X_3$	carrier concentrations (% w/w)
$X_4$	surfactant concentration (% w/w)
$X_5$	pH of the feed phase
$X_6$	agitation speed (rpm)
$X_7$	treat ratio
$X_8$	internal to organic phase ratio

### Acknowledgement

The authors are grateful to University of Malaya, Malaysia for providing the fund to carry out this research work.

### References

- [1] M. Chiha, M.H. Samar, O. Hamdaoui, Extraction of chromium (VI) from sulphuric acid aqueous solutions by a liquid surfactant membrane (LSM), *Desalination* 194 (2006) 69–80.
- [2] A. Zouhri, B. Ernst, M. Burgard, Bulk liquid membrane for the recovery of chromium(VI) from a hydrochloric acid medium using dicyclohexano-18-crown-6 as extractant-carrier, *Sep. Sci. Technol.* 34 (1999) 1891–1905.
- [3] G. Arslan, A. Tor, H. Muslu, M. Ozmen, I. Akin, Y. Cengeloglu, M. Ersoz, Facilitated transport of Cr(VI) through a novel activated composite membrane containing Cyanex 923 as a carrier, *J. Membr. Sci.* 337 (2009) 224–231.
- [4] A. Agrawal, C. Pal, K.K. Sahu, Extractive removal of chromium (VI) from industrial waste solution, *J. Hazard. Mater.* 159 (2008) 458–464.
- [5] N.N. Li, Separating Hydrocarbons with Liquid Membranes, U.S. Patent 3,410,794 (1968).
- [6] R. Ali Kumbasar, Extraction of chromium (VI) from multicomponent acidic solutions by emulsion liquid membranes using TOPO as extractant, *J. Hazard. Mater.* 167 (2009) 1141–1147.
- [7] R.A. Kumbasar, Selective separation of chromium (VI) from acidic solutions containing various metal ions through emulsion liquid membrane using triethylamine as extractant, *Sep. Purif. Technol.* 64 (2008) 56–62.
- [8] S.A. Cavaco, S. Fernandes, M.M. Quina, L.M. Ferreira, Removal of chromium from electroplating industry effluents by ion exchange resins, *J. Hazard. Mater.* 144 (2007) 634–638.
- [9] P.S. Kulkarni, S. Mukhopadhyay, M.P. Bellary, S.K. Ghosh, Studies on membrane stability and recovery of uranium (VI) from aqueous solutions using a liquid emulsion membrane process, *Hydrometallurgy* 64 (2002) 49–58.
- [10] C.C. Lin, R.L. Long, Removal of nitric acid by emulsion liquid membrane: experimental results and model prediction, *J. Membr. Sci.* 134 (1997) 33–45.
- [11] H.R. Mortaheb, H. Kosuge, B. Mokhtarani, M.H. Amini, H.R. Banihashemi, Study on removal of cadmium from wastewater by emulsion liquid membrane, *J. Hazard. Mater.* 165 (2009) 630–636.
- [12] J.D. Holbrey, K.R. Seddon, *Ionic Liquids. Clean Products and Processes*, vol. 1, 1999, pp. 223–237.
- [13] M.J. Earle, K.R. Seddon, *Ionic liquids. Green solvents for the future*, *Pure Appl. Chem.* 72 (7) (2000) 1391–1398.
- [14] K. Mikami, *Green Reaction Media in Organic Synthesis*, first ed., Blackwell, UK, 2005.

- [15] T. Welton, Room-temperature ionic liquids. Solvents for synthesis and catalysis, Chem. Rev. 99 (1999) 2071–2083.
- [16] P. Wasserscheid, T. Welton, Ionic Liquids in Synthesis, second ed., Wiley-VCH, Weinheim, 2008.
- [17] M. Freemantle, New horizons for ionic liquids, Chem. Eng. News 79 (2001) 21–25.
- [18] C.J. Adam, M.J. Earle, G. Robert, K.R. Seddon, Friedel–Crafts reactions in room temperature ionic liquids, Chem. Commun. 19 (1998) 2097–2098.
- [19] P.J. Dyson, D.J. Ellis, D.C. Parker, T. Welton, Arene hydrogenation in a room-temperature ionic liquid using a ruthenium cluster catalyst, Chem. Commun. 1 (1999) 25–26.
- [20] C.E. Song, E.J. Roh, Practical method to recycle a chiral (salen)Mn epoxidation catalyst by using an ionic liquid, Chem. Commun. 10 (2000) 837–838.
- [21] A.E. Visser, R.P. Swatloski, W.M. Reichert, R. Mayton, S. Sheff, A. Wierzbicki, J.H. Davis Jr., R.D. Rogers, Task-specific ionic liquids for the extraction of metal ions from aqueous solutions, Chem. Commun. 1 (2001) 135–136.
- [22] A.P. de los Rios, F.J. Hernandez-Fernandez, L.J. Lozano, S.S. nchez, M.J.I.C. Godnez, Removal of metal ions from aqueous solutions by extraction with ionic liquids, J. Chem. Eng. Data 55 (2010) 605–608.
- [23] A.E. Visser, R.P. Swatloski, W.M. Reichert, S.T. Griffin, R.D. Rogers, Traditional extractants in nontraditional solvents: group 1 and 2 extraction by crown ethers in room-temperature ionic liquids, Ind. Eng. Chem. Res. 39 (10) (2000) 3596–3604.
- [24] S. Dai, Y.H. Ju, C.E. Barnes, Solvent extraction of strontium nitrate by a crown ether using room temperature ionic liquids, J. Chem. Soc. Dalton Trans. (1999) 1201–1202.
- [25] L.C. Branco, J.G. Crespo, C.A.M. Afonso, High selective transport of organic compounds by using supported liquid membranes based on ionic liquids, Angew. Chem. Int. Ed. 41 (2002) 2771–2773.
- [26] A.G. Fadeev, M.M. Meagher, Opportunities for ionic liquids in recovery of bio-fuels, Chem. Commun. 3 (2001) 295–296.
- [27] I.W. Sun, C.L. Hussey, Electrochemistry of niobium chloride and oxide chloride complexes in the basic aluminum chloride-1-methyl-3-ethylimidazolium chloride room-temperature ionic liquid, Inorg. Chem. 28 (1989) 2731–2737.
- [28] T. Ölmez, The optimization of Cr(VI) reduction and removal by electrocoagulation using response surface methodology, J. Hazard. Mater. 162 (2009) 1371–1378.
- [29] M.S. Bhatti, A.S. Reddy, A.K. Thukral, Electrocoagulation removal of Cr(VI) from simulated wastewater using response surface methodology, J. Hazard. Mater. 172 (2009) 839–846.
- [30] E. Kristo, C.G. Biliaderis, N. Tzanetakis, Modelling of the acidification process and rheological properties of milk fermented with a yogurt starter culture using response surface methodology, Food Chem. 83 (2003) 437–446.
- [31] L.-S.T. Lai, C.-C. Pan, B.-K. Tzeng, The influence of medium design on lovastatin production and pellet formation with a high-producing mutant of *Aspergillus terreus* in submerged cultures, Process Biochem. 38 (2003) 1317–1326.
- [32] E.L. Soo, A.B. Salleh, M. Basri, R.N.Z.A. Rahman, K. Kamaruddin, Response surface methodological study on lipase-catalyzed synthesis of amino acid surfactants, Process Biochem. 39 (2004) 1511–1518.
- [33] S. Mannan, A. Fakhru'l-Razi, M.Z. Alam, Optimization of process parameters for the bioconversion of activated sludge by *Penicillium corylophilum*, using response surface methodology, J. Environ. Sci. 19 (2007) 23–28.
- [34] M. Rajasimman, R. Sangeetha, P. Karthik, Statistical optimization of process parameters for the extraction of chromium(VI) from pharmaceutical wastewater by emulsion liquid membrane, Chem. Eng. J. 150 (2009) 275–279.
- [35] S. Nosrati, N.S. Jayakumar, M.A. Hashim, Extraction performance of chromium(VI) with emulsion liquid membrane by Cyanex 923 as carrier using response surface methodology, Desalination 266 (2010) 286–290.
- [36] M. Rajasimman, R. Sangeetha, Optimization of process parameters for the extraction of chromium (VI) by emulsion liquid membrane using response surface methodology, J. Hazard. Mater. 168 (2009) 291–297.